Electrochemistry of thorium in LiCl-KCl eutectic melts

L. Cassayre, J. Serp, P. Soucek, R. Malmbeck*, J. Rebizant, J.-P. Glatz

European Commission, JRC, Institute for Transuranium Elements, P.O. 2340,

76125 Karlsruhe, Germany

Abstract

This work presents a study of the electrochemical properties of Th chloride ions dissolved in a molten LiCl-KCl eutectic, in a temperature range of 693-823 K. Transient electrochemical techniques such as cyclic voltammetry and chronopotentiommetry have been used in order to investigate the reduction mechanism on a tungsten electrode and the diffusion coefficient of dissolved Th ions. All techniques showed that only one valence state was stable in the melt. The reduction into Th metal was found to occur according to a one-step mechanism, through an irreversible reaction controlled by a nucleation process which requires an overpotential of several 100 mV. At 723 K, the diffusion coefficient is $D_{Th(723K)} = 3.7 \pm 0.2 \cdot 10^{-5}$ $cm^2.s^{-1}$. EMF measurements indicated that, at 723 K, the standard apparent potential is $E^{*0}_{ThCl_4/Th)}$ (723 K) = -2.582 V vs. Cl_2/Cl^-, and the activity coefficient γ_{ThCl4}(723 K) = $8 \cdot 10^{-3}$ on the mole fraction scale (based on a pure liquid reference state).

Keywords: molten chlorides, thorium, transient electrochemistry, *emf* measurements.

* Corresponding author. Tel.: +49 7247 951 376; fax: +49 7247 95199611;
E-mail adress: rikard.malmbeck@ec.europa.eu

1. INTRODUCTION

Previous work performed in ITU concerned the study of the electrochemical properties of U, Pu, Np and Am cations in a LiCl-KCl eutectic molten salt [1-3]. Transient electrochemical techniques were used to determine the diffusion coefficient of the dissolved actinide ions, as well as their redox potentials. Basic thermochemical properties (Gibbs energy and activity coefficient) were also determined in the 673-823 K temperature range.

The electrochemical behaviour of Th ions dissolved in the same chloride melt is reported in this paper. A literature review indicated that the electrochemical behaviour of dissolved Th was not yet well established in the LiCl-KCl eutectic, mostly because some authors proposed the existence of Th(II) cations [4], while others mentioned that the only stable valence state is Th(IV) [5-6].

An electrochemical study was then performed at different temperatures and concentrations in order to determine the basic properties of Th ions in the chloride melt, and to evaluate the reduction mechanism into Th metal on an inert electrode.

2. EXPERIMENTAL

The experiments, storage and handling of all chemicals were carried out in a glove box in purified Ar atmosphere, equipped with a well-type oven.

Almost one gram of metallic Th was alloyed with 26.5g of Bi and placed in an Al_2O_3 crucible together with 43.9g of LiCl-KCl eutectic (Aldrich 99.99%). The electrolytic bath was prepared by oxidising the Th with a known amount of $BiCl_3$ dissolved in the salt, as described in [1]. Five different Th concentrations (between 0.20 wt% and 1.46 wt%) were prepared by successive additions of $BiCl_3$.

Two or three salt samples of about 100 mg were drawn out at each concentration, dissolved and diluted in nitric acid. The concentration of Th was determined both by ICP-MS and XRF analysis. The data are summarized in Table 1.

The electrochemical measurements (cyclic voltammetry, chronopotentiommetry, chronoamperommetry, open-circuit potential) were carried out with a PAR 273 potentiostat. Inert working electrodes were prepared using 1 mm W wire. The reference electrode was composed of an Ag wire dipped into a LiCl-KCl-AgCl(1wt%) mixture, contained in a Pyrex glass tube. The auxiliary electrode was a 1 mm Mo spiral-wire.

The ohmic resistance of the electrolyte was determined by impedance spectroscopy at 733 K: it was found to be 0.41 Ω, and this value was considered constant on the whole range of temperature (693-823 K). The ohmic drop correction was performed on the chronopotentiograms using the relation:

$$E_{corr}=E_{meas} - R_e.I \qquad \text{(Eq. 1)}$$

where E_{corr} is the IR-corrected potential (V), E_{meas} the measured potential (V), R_e the electrolyte resistance (Ω) and I the applied current (A).

For each concentration, chronopotentiograms and cyclic voltammograms were plotted at five temperatures (693, 733, 773, 798 and 823 K). The W working electrode was cleaned between each measurement by applying a short anodic polarization at a current of 10 mA, until reaching the chlorine evolution potential.

3. RESULTS

3.1 Reduction mechanism

A cyclic voltammogram of the whole electrochemical window recorded on an inert W electrode is shown in Figure 1. The solvent decomposition occurs at about -2.40 V vs. Ag/AgCl on the cathodic side (Li^+ reduction) and +1.25 V vs. Ag/AgCl on the anodic side (Cl^- oxidation). It appears that there is only one redox system due to the presence of Th ions in the melt, attributed to the reduction of Th ions into Th metal. It shows that the reduction of Th ions into metal is a one-step process, and that dissolved Th has only one stable electro-active form in the large electrochemical window of the molten LiCl-KCl eutectic.

The effect of the scan rate on the shape of the cyclic voltammograms is shown in Figure 2. In the whole scan rate range (from 50 $mV.s^{-1}$ to 300 $mV.s^{-1}$), the cathodic peak potential is shifted towards more cathodic potentials with increasing scan rate, indicating that the reaction is irreversible [7]. This was confirmed by the analysis of the peak potential evolution versus the logarithm of the scanning rate at five temperatures, presented in Figure 3, which shows a linear relationship between the cathodic peak potential and the logarithm of the scanning rate. This behaviour is rather unexpected, since most of the other actinides have shown a reversible behaviour at low scan range, typically below 200 $mV.s^{-1}$ [1-3].

In the case of such an irreversible system, the analytical expression of the cathodic peak potential can be written as [7]:

$$E_p = k - \frac{2.303RT}{\alpha n} \log\left(\frac{\alpha n F \upsilon}{RT}\right)^{1/2} \qquad \text{(Eq. 2)}$$

where α is the charge transfer coefficient, n the number of electrons exchanged, ν the scan rate ($V.s^{-1}$) and k a constant (V).

The slope of the lines plotted in the coordinates E_p-logν in Figure 3 then allows to determine the αn value for each concentration. These values were found to be between 3.8 and 1.5, with a strong dependence on the concentration: αn decreases with an increasing concentration of Th in the melt. Since the charge transfer coefficient is in between 0 and 1, this result give a first indication that the stable state for Th ions should be Th(IV). Indeed, $\alpha n=3.8$ with $\alpha<1$ leads to $n\geq4$.

A close-up view of the cathodic peak (Figure 4) shows a cross-over between the direct and the reverse scan. This cross-over is attributed to the irreversibility of the nucleation step in the direct scan, which delays the rise of the cathodic current in the reverse scan. Accordingly, this phenomenon is considered to be the proof of the formation of a new solid phase, here Th metal, at the surface of the electrode [7].

The nucleation process taking place at the tungsten electrode can further be evidenced by potential-step measurements. The shape of the curves presented in Figure 5 is indeed characteristic of a nucleation process. After charging the double layer, the initial regime of each transient is characterized by a decrease in current associated to the formation of the first nuclei on the tungsten electrode (zone I). The current then increases, which correspond to an increase of the active area due to crystal growth (zone II). Finally, the current decreases with time due to diffusion control (zone III).

Chronopotentiograms obtained at 733 K are plotted in Figure 6. Again, there was only one redox system evidenced by chronopotentiommetry. Furthermore, the slight decrease of the potential of the plateau with increasing applied current confirms the irreversibility of the system [7].

3.2 Diffusion coefficient

The diffusion coefficient of Th ions was calculated by two electrochemical techniques in the 693-823 K temperature range.

Using chronopotentiograms, the Sand law [7] was applied assuming a 4-electron transfer reaction:

$$I\sqrt{\tau} = \frac{nFc_{Th}S\sqrt{\Pi D_{Th}}}{2} \qquad \text{(Eq. 3)}$$

where I is the applied current (A), τ the transition time (s), n the number of exchanged electrons, F the Faraday constant ($C.mol^{-1}$), c_{Th} the Th concentration ($mol.cm^{-3}$), S the electrode surface (cm^2) and D_{Th} the diffusion coefficient ($cm^2.s^{-1}$).

For each concentration, the Sand equation was verified through the linearity of the plot of I vs. $\tau^{-1/2}$. An example is given in Figure 7. Using the slope of each line, the diffusion coefficient was determined according to Eq. 3.

The temperature dependence of the diffusion coefficient is plotted in Figure 8 in the coordinates $\log(D_{Th})$-1/T. The data obtained for four concentrations are in fairly good agreement, with an average relative standard deviation of 8%.

Cyclic voltammograms obtained at various sweep rates (between 50 and 200 $mV.s^{-1}$) were also used for determination of the diffusion coefficient. For a totally irreversible system, the relation between sweep rate and diffusion coefficient is expressed by the Delahay equation [7]:

$$\frac{Ip}{\sqrt{\nu}} = 0.496(\alpha n)^{1/2} nF^{3/2} (RT)^{-1/2} SD_{Th}^{1/2} c_{Th} \qquad \text{(Eq. 4)}$$

where Ip is the cathodic peak intensity (A), ν the sweep rate ($V.s^{-1}$), T the temperature (K) and other symbols as defined above.

The average evolution of the diffusion coefficient calculated using Eq. 4 is also plotted in Figure 8. The data obtained from CV measurements are somewhat more scattered than the data from CP, having a relative standard deviation of 15%.

An average linear regression of all data was performed to determine the evolution of the diffusion coefficient, according to the Arrhenius law:

$$\log D_{Th} = -1.864 - 1856/T \qquad \text{(Eq. 5)}$$

At 723 K, the diffusion coefficient is: $D_{Th(723\ K)} = 3.7 \pm 0.2 \cdot 10^{-5}\ cm^2.s^{-1}$.

This value is in the same order of magnitude as others determined for actinides (U, Pu, Np, Am) in the LiCl-KCl eutectic melt [8], but one order of magnitude higher than published by Martinot [5] in the case of Th.

3.3 Apparent standard potential and activity coefficient

Since the system was found to be irreversible because of a nucleation process, it was difficult to establish the apparent standard potential of the system with transient electrochemical techniques. EMF measurements were then performed to determine the apparent standard potential. For each temperature and concentration, the tungsten electrode was coated with Th metal by application of a cathodic current for 60s, and the open-circuit potential (OCP) was

recorded versus the Ag/AgCl reference electrode. A very stable plateau was obtained each time, allowing the measurement of the corresponding equilibrium potential E^{eq}.

The measured equilibrium potential for a pure metal in equilibrium with its chloride is given by the Nernst law:

$$E^{eq}_{Th(IV)/Th(0)}\,(VvsAg/AgCl) = E^{0}_{Th(IV)/Th(0)} + \frac{2.303RT}{nF}\log\frac{a_{Th(IV)}}{a_{Th(0)}} \qquad \text{(Eq. 6)}$$

where $E^{0}_{Th(IV)/Th(0)}$ is the standard potential at a hypothetical supercooled liquid reference state of unit mole fraction and unit activity, $a_{Th(IV)}$ and $a_{Th(0)}$ are the activity of Th ions and of metallic Th, respectively. Unit activity was assumed for pure metal.

The apparent standard potential, $E^{*0}_{Th(IV)/Th(0)}$ of the Th redox couple is defined as:

$$E^{*0}_{Th(IV)/Th(0)} = E^{0}_{Th(IV)/Th(0)} + \frac{2.303RT}{nF}\log\gamma_{Th(IV)} \qquad \text{(Eq. 7)}$$

where $\gamma_{Th(IV)} = \frac{a_{Th(IV)}}{X_{Th(IV)}}$ is the activity coefficient of Th and $X_{Th(IV)}$ is the molar fraction of Th in the salt.

Combining Eq. 6 and Eq. 7, $E^{eq}_{Th(IV)/Th(0)}$ can be expressed as:

$$E^{eq}_{Th(IV)/Th(0)} = E^{*0}_{Th(IV)/Th(0)} + \frac{2.303RT}{nF}\log X_{Th(IV)} \qquad \text{(Eq. 8)}$$

A linear fit of the plots of E^{eq} vs. $\log(X_{Th})$ (Figure 9) identified to Eq. 8 allows then to determine $E^{*0}_{Th(IV)/Th(0)}$ and n.

Firstly, the number of electrons of the redox system was calculated according to the slope of the lines: an average value of n = 4.17 was obtained, which confirms that there is only one stable state of Th chloride in the melt, i.e. Th(IV).

Secondly, the zero-intercept of the lines ($\log(X_{Th})=0$) gives a value of $E^{*0}_{Th(IV)/Th(0)}$ for each temperature, as summarized in Table 2. For the purpose of comparison with literature data, the potential data have been calculated vs. the Cl_2/Cl^- reference electrode as detailed in [1], according to Eq. 9:

$$E_{Ag/AgCl}\,(V vs Cl_2/Cl^-) = E^0_{AgCl} + \frac{2.303RT}{F}\log X_{AgCl} \qquad \text{(Eq. 9)}$$

with $X_{AgCl}=0.0039$ (1wt%)

$E^0_{AgCl} = -1.0910 + 2.92410^{-3}T(K)$ according to [6, 9].

The data of apparent standard potential are plotted vs. temperature in Figure 10 and compared to tabulated data from Smirnov [10] and Yang [6]. The agreement is fairly good, with a discrepancy of less than 40 mV between the different set of data.

A linear fit of the apparent standard potentials established in this work gives:

$E^{*0}_{Th(IV)/Th(0)}$ (V vs. Cl_2/Cl^-) = - 2.983 + 5.54·10^{-3} T (K) (Eq. 10)

The activity coefficient $\gamma(ThCl_4)$ was determined according to Eq. 7, using our experimental data for $E^{*0}_{Th(IV)/Th(0)}$ and tabulated data for $E^0_{Th(IV)/Th(0)}$. The standard potential $E^0_{Th(IV)/Th(0)}$ was calculated from tabulated Gibbs energy data from [11] according to Eq. 11:

$$E^0_{Th(IV)/Th(0)} = \frac{\Delta G^{\circ}_{f(sc)}}{4F} \qquad \text{(Eq. 11)}$$

where $\Delta G^{\circ}_{f(sc)}$ is the standard Gibbs energy of formation of $ThCl_4$ in the liquid state at the relevant temperature ($J.mol^{-1}$).

In the 693-823 K temperature range, the activity coefficient is rather low (~$5 \cdot 10^{-4}$, see Table 2Table 2), which confirms recent Raman spectra studies [12] showing a strong tendency of Th(IV) to form chloride complexes in chloride melts.

4. CONCLUSIONS

This electrochemical study of Th ions in a LiCl-KCl eutectic melt indicates that there is only one stable electro-active species in the 693-823 K temperature range and in the 0.20-1.46 wt% concentration range. The temperature dependence of the potential of metallic Th in equilibrium with its ions indicates that this stable species is Th(IV).

The electrochemical reduction of Th(IV) to Th metal occurs as an irreversible reaction. The nucleation process of Th metal induces an overpotential of several 100 mV. By using *emf* measurements, the standard apparent potential was found to be $E^{*0}_{ThCl_4/Th)}$ (723 K) = -2.582 V vs. Cl_2/Cl^-, and the activity coefficient on the mole fraction scale $\gamma_{ThCl4}(723\ K) = 5 \cdot 10^{-4}$.

At 723 K, the diffusion coefficient is $D_{Th(723K)} = 3.7 \pm 0.2 \cdot 10^{-5}$ $cm^2.s^{-1}$, and this coefficients dependence on temperature follows the Arrhenius law.

Acknowledgments

The authors wish to thank B.Lynch for XRF measurements as well as C.Scheppler, S.Birck and S.v.Winckel for ICP-MS analysis. This work was carried out with the European Commission financial support in the 6th framework program, under the contract FI6W-CT-2003-408854, "EUROPART".

References

[1] J. Serp, R.J.M. Konings, R. Malmbeck, J. Rebizant, C. Scheppler, J.-P. Glatz, J. Electroanal. Chem., 561 (2004) 143.

[2] P. Masset, D. Bottomley, R.J.M. Konings, R. Malmbeck, A. Rodriguez, J. Serp, J.-P. Glatz, J. Electrochem. Soc., 152(6) (2005) 1109.

[3] J. Serp, P. Chamelot, S. Fourcaudot, R.J.M. Konings, R. Malmbeck, C. Pernel, J.C. Poignet, J. Rebizant and J.-P. Glatz, Electrochim. Acta, 51(19) (2006) 4024.

[4] T. Yanagi, K. Sakoda, K. Tsuji, Technology Reports of the Osaka University, 28(1428) (1978) 319.

[5] L. Martinot, J. Radioanal. Nucl. Chem. Lett., 103(6) (1986) 357.

[6] L. Yang, R.G. Hudson, C.-Y Chien, Phys. Chem. Process Metallurgy, (1961) 925.

[7] A. J. Bard, L. R. Faulkner, Electrochemical methods – Fundamentals and applications, John Wiley & Sons, New York, 1980.

[8] P. Masset, R.J.M. Konings, R. Malmbeck, J. Serp and J.-P. Glatz, J. Nucl. Mater., 344(1-3) (2005) 173.

[9] S.P. Fusselman, J.J. Roy, D.L. Grimmett, L.F. Grantham, C.L. Krueger, C.R. Nabelek, T.S. Storvick, T. Inoue, T. Hijikata, K. Kinoshita, Y. Sakamura, K. Uozumi, T. Kawai, N. Takahashi, J. Electrochem. Soc., 146(7) (1999) 2573.

[10] M.V. Smirnov, Electrode Potentials in Fused Chlorides (Elektrodnye Potentsialy v Rasplavlennykh Khloridakh), Nauka, Moscow, 1973.

[11] J. Fuger, V.B. Parker, W.N. Hubbard, F.L. Oetting, The chemical thermodynamics of actinide elements compounds. Part 8: The actinide halides, IAEA, Vienna, 1983.

[12] G.M. Photiadis and G.M. Papatheodorou, J. Chem. Soc., Dalton Trans. (1999) 3541.

Figures captions

Figure 1: Cyclic voltammogram obtained on a W electrode (S=0.31 cm^2) in a melt containing 0.43 wt.% of $ThCl_4$ in the LiCl-KCl eutectic, T=773 K, scan rate = 100 $mV.s^{-1}$.

Figure 2: Cyclic voltammograms (scan rate from 50 to 300 $mV.s^{-1}$) obtained on a W electrode (S=0.31 cm^2) in a melt containing 0.43 wt.% of $ThCl_4$ in the LiCl-KCl eutectic, T=733 K.

Figure 3: Evolution of the potential of the cathodic peak (Ec) with the logarithm of the scan rate for cyclic voltammograms obtained on a W electrode (S=0.31 cm^2), at five temperatures, in a melt containing 0.43 wt.% of $ThCl_4$ in the LiCl-KCl eutectic.

Figure 4: Cyclic voltammogram illustrating the 'nucleation cross-over effect' on the reverse scan for Th deposition on a W electrode (S=0.31 cm^2) in a melt containing 0.96 wt.% of $ThCl_4$ in the LiCl-KCl eutectic, T=733 K, scan rate = 100 $mV.s^{-1}$.

Figure 5: Potentiostatic current-time plots corresponding to Th deposition on a W electrode (S=0.31 cm^2) in a melt containing 0.20 wt.% of $ThCl_4$ in the LiCl-KCl eutectic, T=733 K, at two potentials (1: -1.54 V, 2: -1.60 V).

Figure 6: Chronopotentiograms (corrected for ohmic drop) obtained on a W electrode (S=0.31 cm^2) in a melt containing 0.43 wt.% of $ThCl_4$ in the LiCl-KCl eutectic, T=733 K.

Figure 7: Verification of the Sand equation for chronopotentiograms obtained on a W electrode (S=0.31 cm^2) in a melt containing 0.43 wt.% of $ThCl_4$ in the LiCl-KCl eutectic.

Figure 8: Diffusion coefficient of Th(IV) dissolved in LiCl-KCl as function of inverse temperature, according to two transient electrochemical techniques (Chronopotentiommetry-CP and Cyclic Voltammetry-CV).

Figure 9: Evolution of the equilibrium potential E^{eq} with the molar fraction of Th(IV) for five temperatures in the LiCl-KCl eutectic.

Figure 10: Comparison of the apparent standard potential of Th(IV)/Th(0) in the LiCl-KCl eutectic; ▲ this work; □ Smirnov [10]; ◊ Yang [6].

Tables

Units	Th concentrations				
wt%	0.96	0.20	0.43	1.46	0.74
mol.cm^{-3}	6.85E-05	1.39E-05	3.05E-05	1.04E-04	5.26E-05
molar fraction	2.30E-03	4.68E-04	1.03E-03	3.48E-03	1.77E-03

Table 1: Th concentration in the LiCl-KCl melt (determined by ICP-MS and XRF).

	Temperature/K				
Potential /V	693	733	773	798	823
$E^{*0}_{Th(IV)/Th(0)}$ vs. Ag/AgCl	-1.380	-1.350	-1.325	-1.296	-1.287
$E^{*0}_{Th(IV)/Th(0)}$ vs. Cl_2/Cl^-	-2.599	-2.577	-2.559	-2.534	-2.530
$E^{0}_{Th(IV)/Th(0)}$ vs. Cl_2/Cl^-	-2.481	-2.457	-2.433	-2.419	-2.404
$10^4.\gamma(ThCl_4)$	3.7	5.0	6.8	8.1	9.6

Table 2: Apparent standard potential E*° derived from OCP measurements, standard potential E° calculated from tabulated data [11] and calculated activity coefficient of $ThCl_4$ in the LiCl-KCl eutectic.

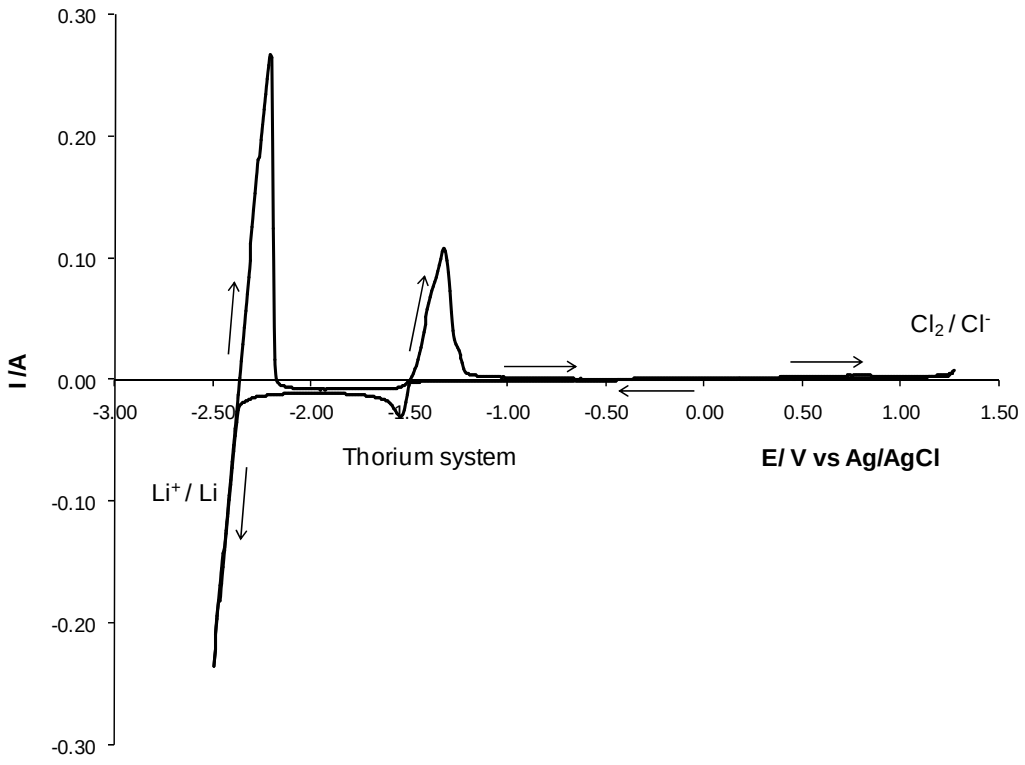

Figure 1

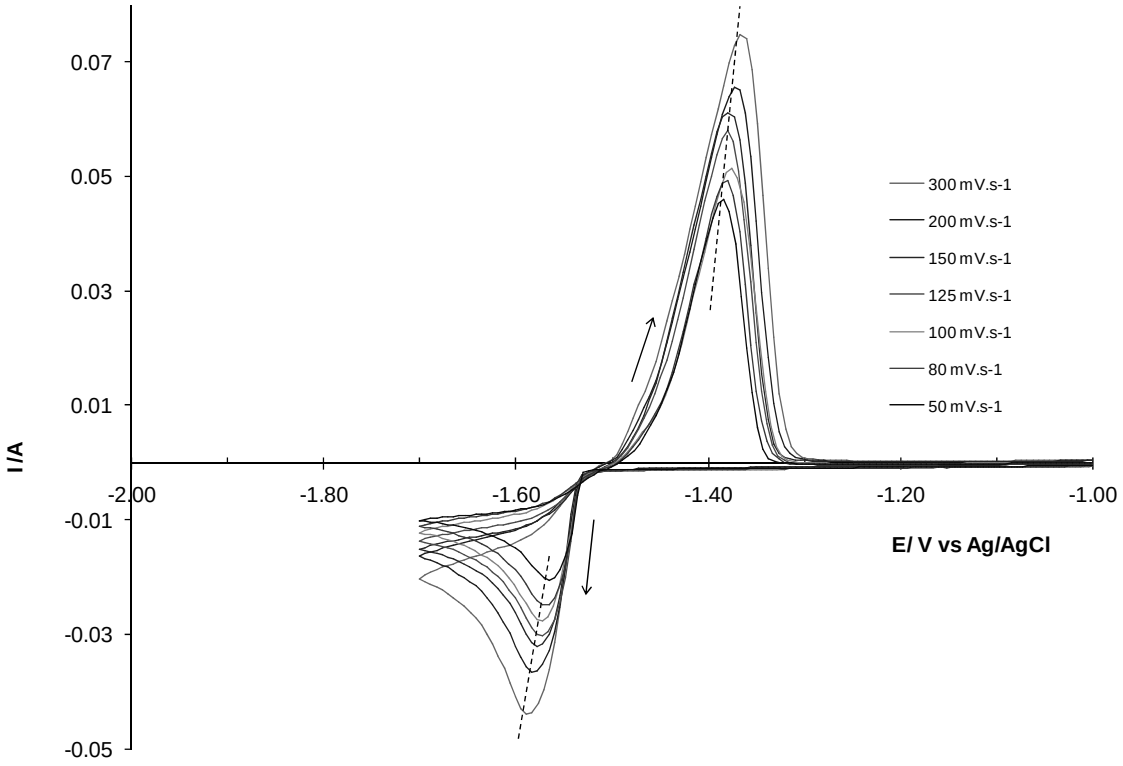

Figure 2

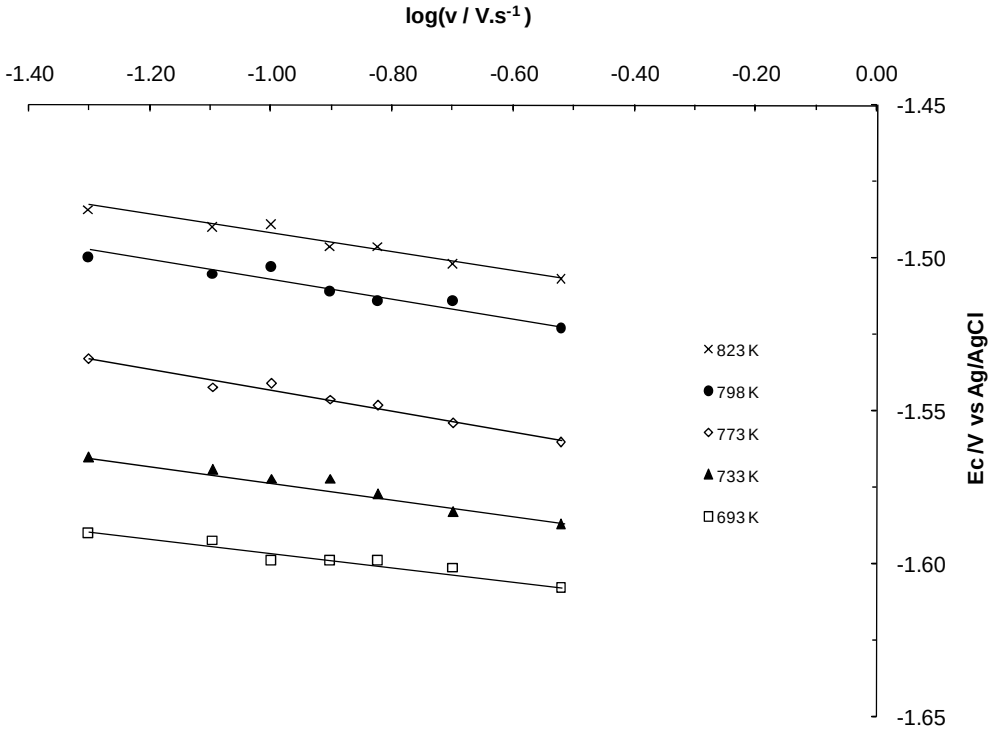

Figure 3

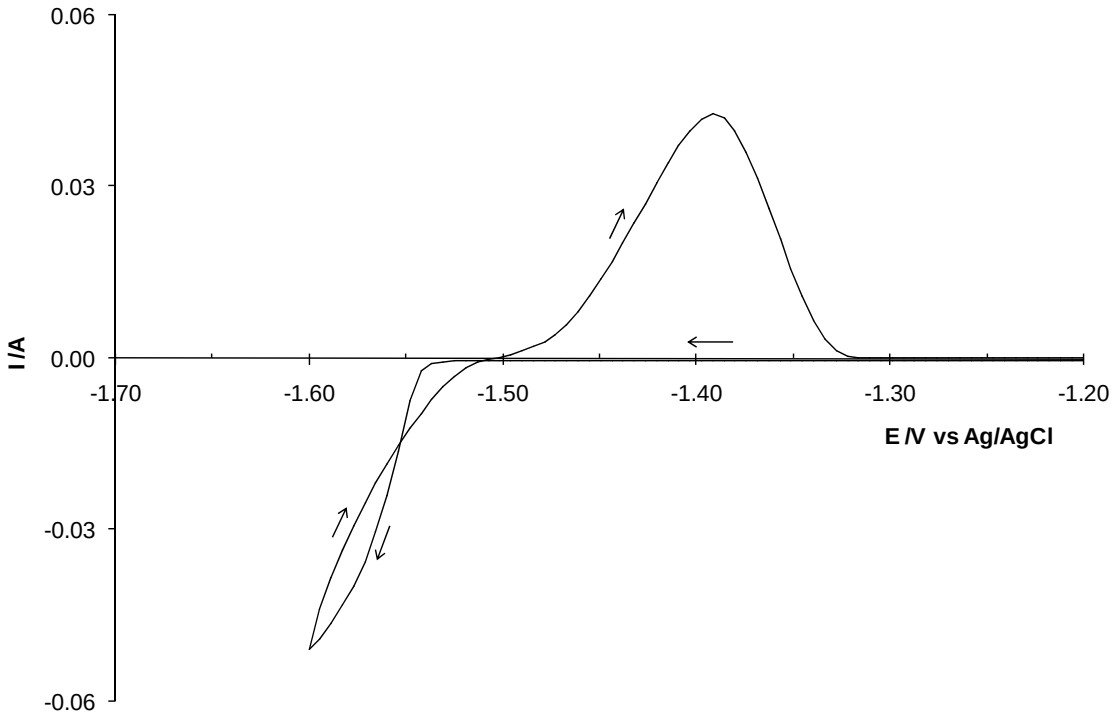

Figure 4

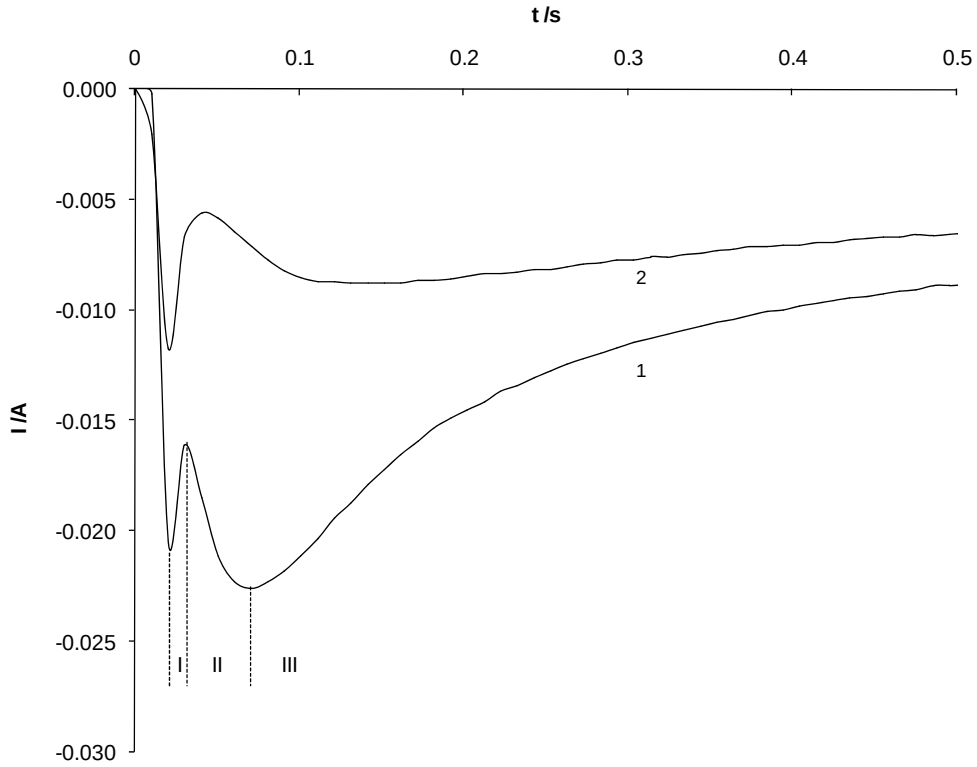

Figure 5

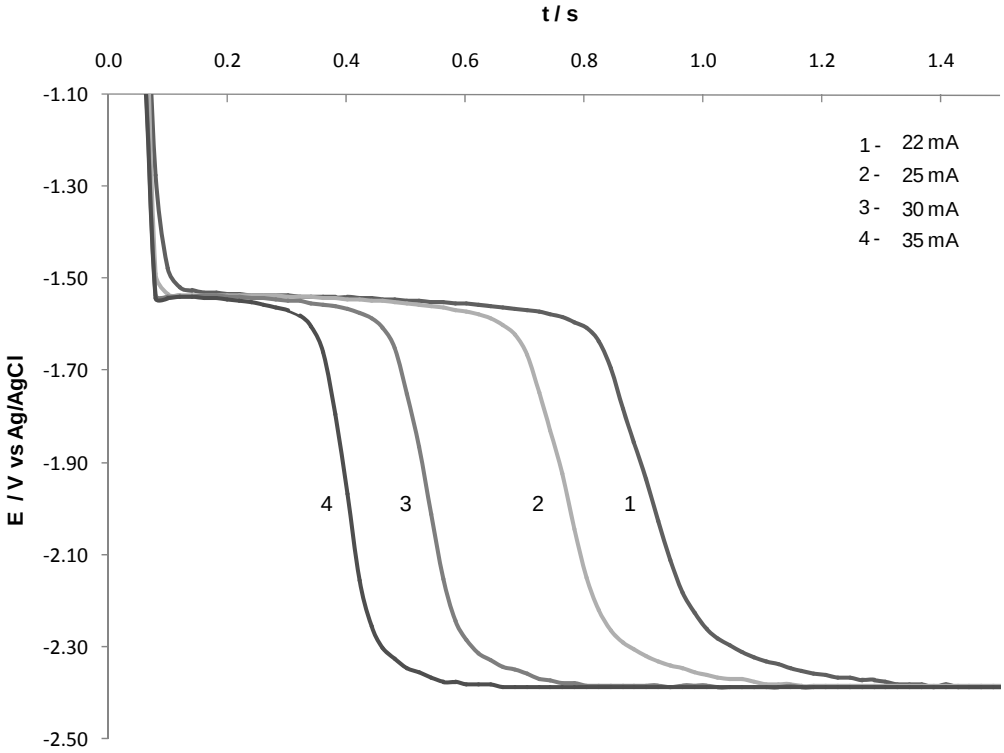

Figure 6

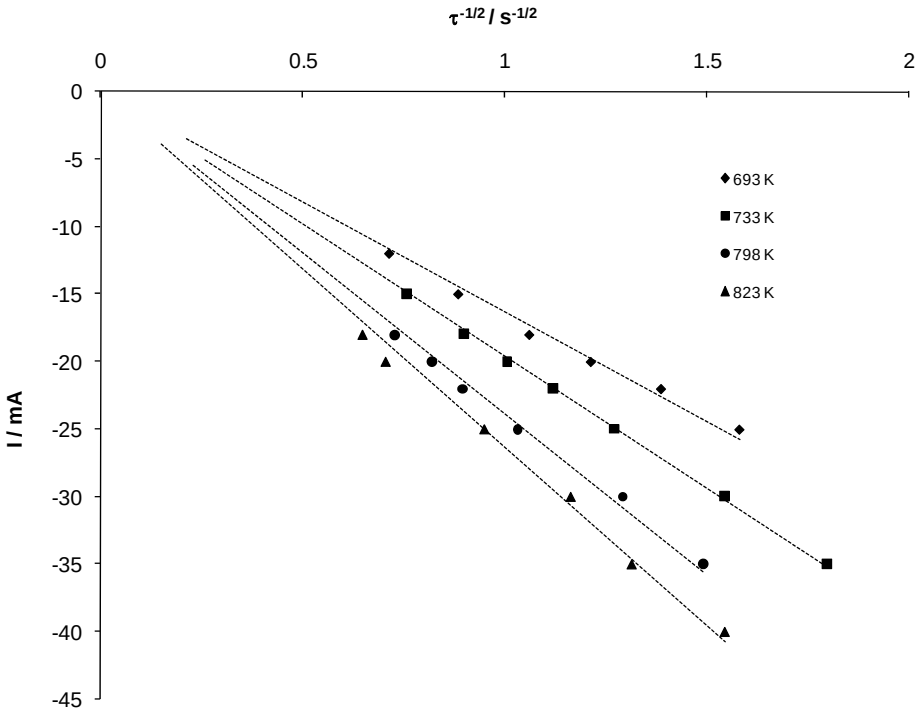

Figure 7

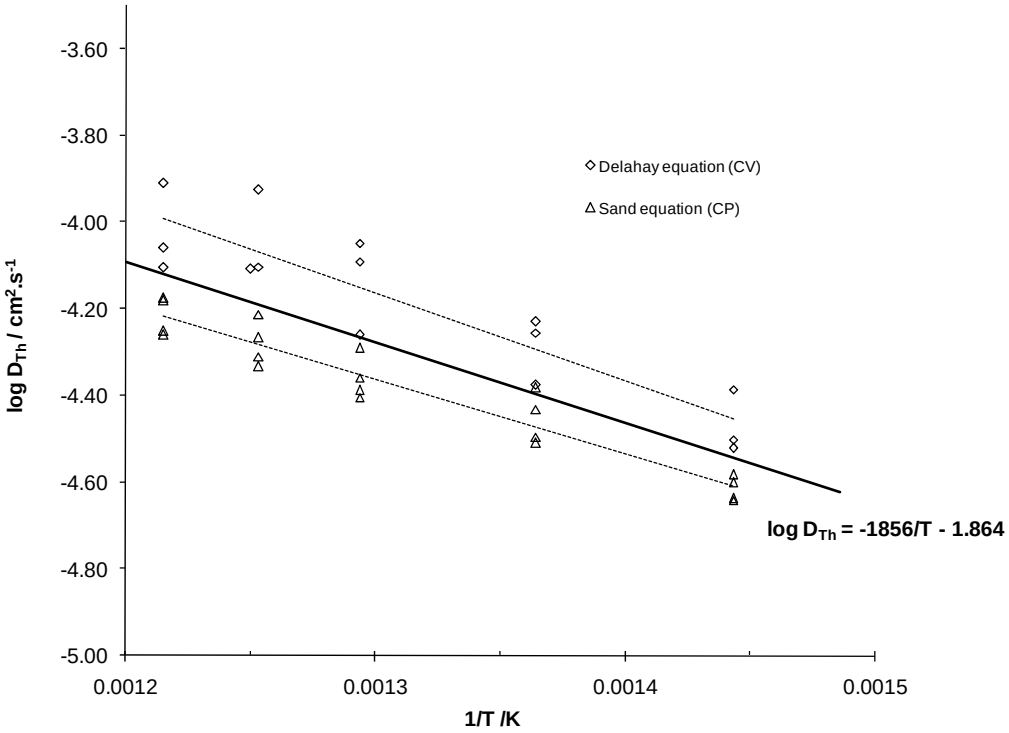

Figure 8

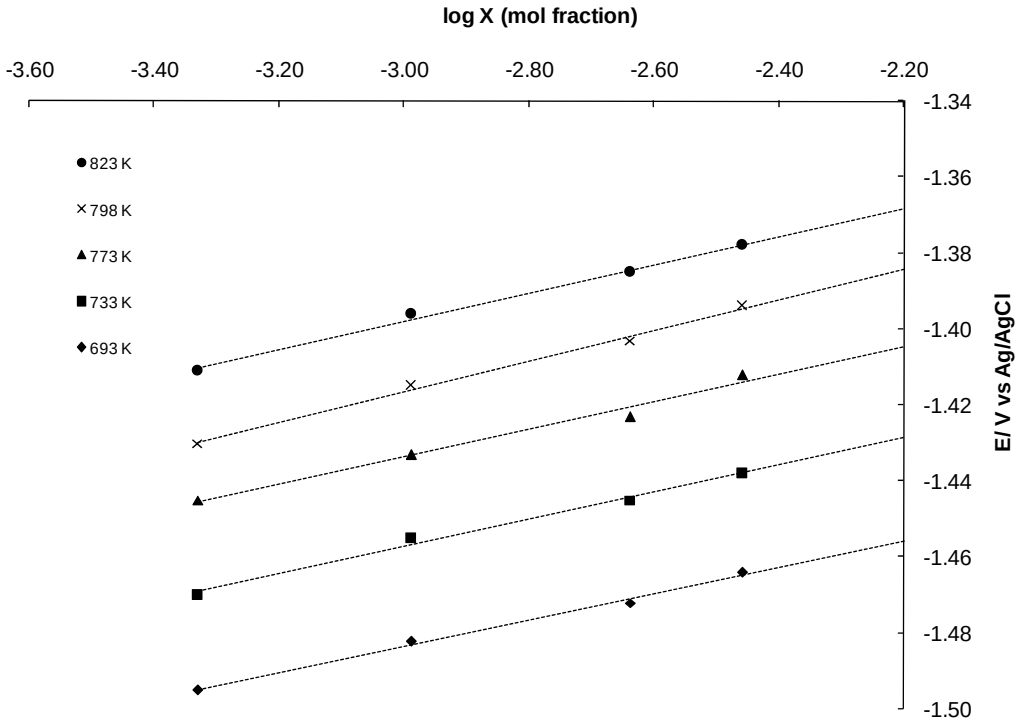

Figure 9

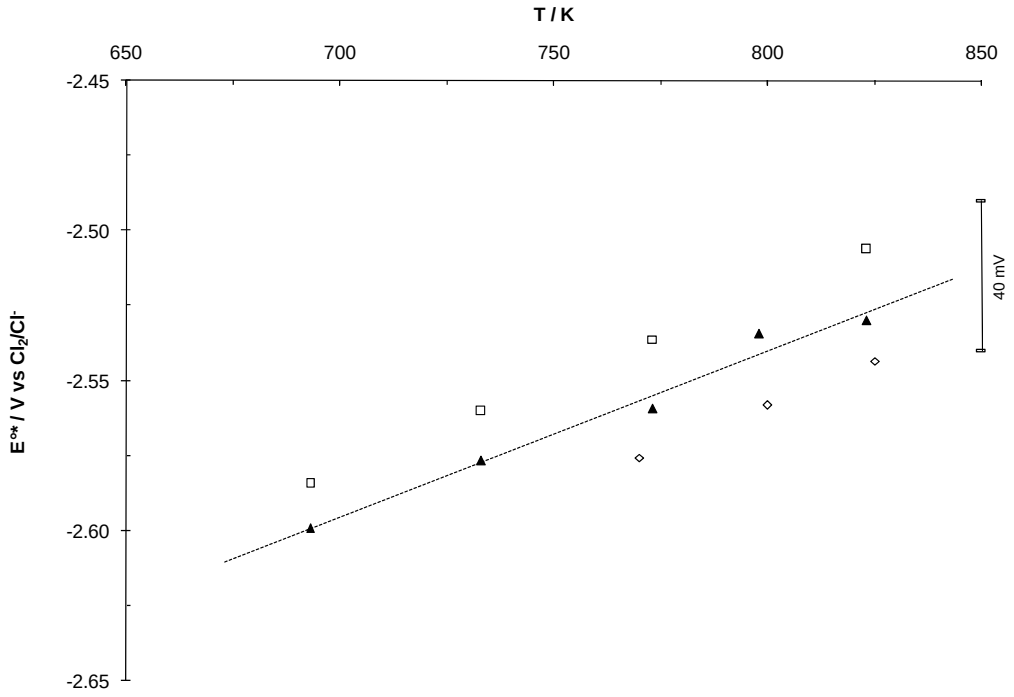

Figure 10